Desalination and Water Treatment
www.deswater.com

doi:10.5004/dwt.2017.20191

72 (2017) 207–215
April

Enantioseparation of (S)-amlodipine from pharmaceutical wastewater by hollow-fiber supported liquid membrane: central composite design and optimization

Niti Sunsandee[a], Naphaphan Kunthakudee[b], Boonta Chutvirasakul[c], Suphot Phatanasri[a,*], Prakorn Ramakul[b,*]

[a]*Department of Chemical Engineering, Faculty of Engineering, Chulalongkorn University, Bangkok 10330, Thailand, Tel. +662-218-6890, Fax +662-218-6877, email: s_phatanasri@yahoo.com (S. Phatanasri)*
[b]*Department of Chemical Engineering, Faculty of Engineering and Industrial Technology, Silpakorn University, Nakhon Pathom 73000, Thailand, Tel. +6681-682-2105, Fax +6634-219-368, email: p_ramakul@su.ac.th (P. Ramakul)*
[c]*Department of Pharmaceutical Chemistry, Faculty of Pharmacy, Srinakharinwirot University, Nakhon Nayok 26120, Thailand*

Received 22 May 2016; Accepted 21 August 2016

ABSTRACT

The enantioseparation of (*S*)-amlodipine and (*R*)-amlodipine from pharmaceutical wastewater by hollow fiber supported liquid membrane was examined. The pH effects of feed solution, concentration of (+)-DBTA, temperature and the flow rates of feed and stripping solution were investigated. A central composite design (CCD) was used for the design of experiment and to determine the significant factors and their interactions. Regression equations were created from the CCD to predict the percentages of extraction and stripping with varying factor levels. The validity of the model was evaluated, and the optimized condition determined by response surface methodology. The highest extraction and stripping performances were 82.0 and 76.0%, respectively.

Keywords: (*S*)-amlodipine; Enantioseparation; Liquid membrane; Hollow fiber

1. Introduction

Amlodipine is a drug in a class of calcium channel blocker (CCB), used to treat high blood pressure (hypertension) and reduce chest pain (angina) [1]. Amlodipine consists of (*S*)-amlodipine (Fig. 1a) and (*R*)-amlodipine (Fig. 1b). Essentially, the calcium channel blocking effect is confined to (*S*)-amlodipine, whereas (*R*)-amlodipine exhibits a much lower calcium channel blocking activity. (*S*)-amlodipine is a more potent showing about 2000 times the potency in *in vitro* evaluation in the rat aorta than the (*R*)-amlodipine [2]. (*S*)-amlodipine provides longer duration of action which reduces the chances of reflex tachycardia [3]. The enantioseparation of (*S*)-amlodipine from its racemate is a very challenging research area. Several researchers dedicated to the separation of amlodipine have been reported. Gotrane et al. [4] separated diastereomers by salt crystallization, however, this required a long time with multiple steps and led to considerable loss of product. Streel et al. [5] and Luksa et al. [6] used chromatographic techniques, and Zandkarimi et al. [7] used capillary electrophoresis. The common preparation of (*S*)-amlodipine follows the selective diastereomeric salt crystallization method. Unfortunately, this separation process has some serious disadvantages. The technique requires a considerable number of different steps and is not suitable for production of multi-gram-quantities. It is also time consuming and expensive. Asymmetric synthesis and kinetic resolution have been developed, but the costs of these processes are high and require a long operating time to develop a proper route for all the chiral compounds.

*Corresponding author.

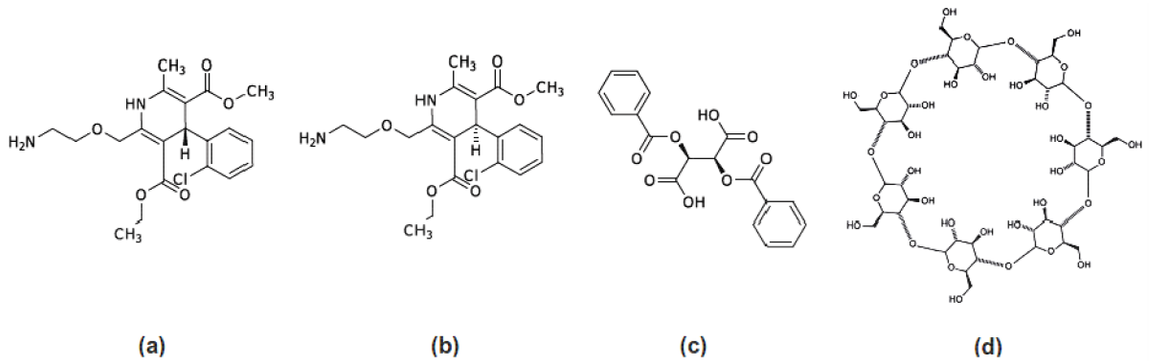

Fig. 1. The structure of (a) (*S*)-amlodipine; (b) (*R*)-amlodipine; (c) O,O′-dibenzoyl-(2*S*,3*S*)-tartaric acid; (d) β-cyclodextrin.

Attempts were made to overcome these problems and separate (*S*)-amlodipine from its racemate. Liquid membrane is considered an effective technique for the simultaneous extraction and recovery of target component from a very dilute solution in a feed by a single unit operation [8]. The membranes contain an extractant or a carrier. The solute can be transferred from low to high concentration because the extractant has the potential for selective permeation using the facilitated transport mechanism [8]. There are two types of liquid membranes, emulsion liquid membrane (ELM) and supported liquid membrane (SLM). ELM has a high transport area [9] and solute extraction is fast. However, the recovery process of the concentrated solute (demulsification) is complicated, and ELM suffers from swelling instability. These factors make the ELM technique commercially uneconomical.

In SLMs, the liquid membrane is held in a porous structure, usually in a porous polyethylene. There are many types of SLM including flat sheet, spiral and hollow fiber. The advantages of hollow fiber supported liquid membranes include a lower amount of extractant used than required in solvent extraction, long life time, low energy consumption and high selectivity [10–12]. Therefore, the hollow fiber supported liquid membrane (HFSLM) was used to separate (*S*)-amlodipine and (*R*)-amlodipine from pharmaceutical wastewater. Liquid membranes have been widely applied to the extraction and recovery of metal ions [13–15], organic compounds [16] and enzymatic transformation. In our previous work, the separation of (*S*)-amlodipine by hollow fiber supported liquid membrane with promising results [17]. (+)-DBTA selectively reacted with (*S*)-amlodipine to form complexes by hydrogen bonding, while (*R*)-amlodipine does not and would be remained in the feed solution.

This study investigated optimizing the separation of (*S*)-amlodipine with HFSLM from pharmaceutical wastewater. Central composite design (CCD) is a systematic concept for the planning and execution of informative experiments. The effects of various factors including pH of the feed solution, temperature, concentration of (+)-DBTA, and flow rates of the feed and stripping solutions were investigated. The main effect and interaction effect of these parameters were determined. Consequently, regression models were developed by response surface methodology which correlated with the significant factors to optimize the extraction and stripping of (*S*)-amlodipine.

2. Separation mechanism of *(S)*-amlodipine in hollow fiber module

A hollow fiber supported liquid membrane system consists of an aqueous feed phase, an organic liquid membrane phase, and an aqueous stripping phase (Fig. 2). The feed and stripping phases were in contact with the organic membrane phase, while the liquid membrane phase which contained an extractant was held in polymeric micropores by capillary force [8]. In this work, the feed solution contained racemic amlodipine, and the liquid membrane had (+)-DBTA as an enantioselector dissolved in 1-decanol. The enantioselective extraction procedure of amlodipine was as follows. The enantioselector, (+)-DBTA would reacted with (*S*)-amlodipine in the feed phase to form a complex of (*S*)-amlodipine$_2$ · (+)-DBTA by hydrogen bonding as described in Eq. (1) [18].

$$2[(S)\text{-Amlodipine} + [(+)\text{-DBTA}] \leftrightarrow [(S)\text{-amlodipine}]_2 \cdot (+) - \text{DBTA} \quad (1)$$

This complex [(*S*)-amlodipine]$_2$ · (+)-DBTA diffused across the membrane phase to the opposite side due to the concentration gradient, and reacted with β-cyclodextrin as the stripping agent. Finally, (*S*)-amlodipine was released into the stripping phase by the reaction shown in Eq. (2). The transport mechanism of (*S*)-amlodipine through the liquid membrane is also shown in Fig. 2.

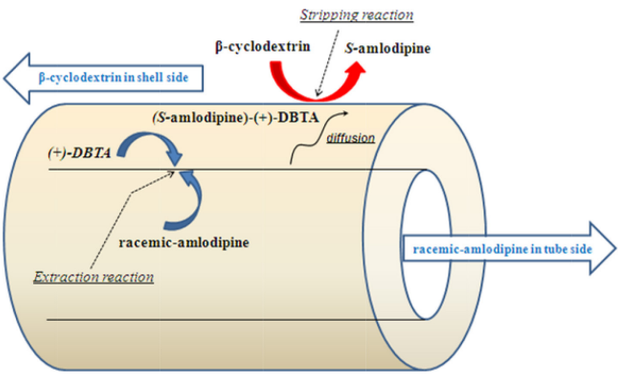

Fig. 2. Transport scheme for chiral extraction.

$$[(S)\text{-amlodipine}]_2 \cdot (+)-\text{DBTA} + 2[\beta-\text{cyclodextrin}] \leftrightarrow 2[(S)\text{-amlodipine}] \cdot [\beta-\text{cyclodextrin}] + [(+)-\text{DBTA}] \quad (2)$$

3. Experimental

3.1. Chemicals and reagents

Wastewater containing 4 mmol/L of racemic amlodipine was taken from a chemical synthesis-based amlodipine pharmaceutical plant of the Government Pharmaceutical Organization (GPO), Bangkok, Thailand. (+)-DBTA (O,O′-dibenzoyl-(2S,3S)-tartaric acid) and β-cyclodextrin were purchased from Acros Organics (Geel, Belgium). Analytical grade 1-decanol was used as the diluent.

3.2. Apparatus

- A Liqui-Cel® Laboratory Liquid/Liquid Extraction System (composed of two gear pumps, two variable speed controllers, two rotameters and four pressure gauges) was used.
- A Liqui-Cel® Extra-Flow module (Celgard, Charlotte, NC; formerly Hoechst Celanese) was used as a support material. This module uses Celgard® microporous polyethylene fibers woven into a fabric and wrapped around a central tube feeder that supplies the shell-side fluid. The woven fabric allows more uniform fiber spacing, which in turn leads to higher mass transfer coefficients than those obtained with individual fibers. The properties of the hollow fiber module are shown in Table 1. The fibers were potted into a solvent-resistant polyethylene tube sheet with a polypropylene shell casing.
- High performance liquid chromatography (HPLC)

3.3. Procedures

The single-module operation is shown in Fig. 3. The liquid membrane, the solution between (+)-DBTA and 1-decanol, was pumped into the tube and shell sides of the hollow fiber module for 20 min to ensure that the liquid membrane was fully embedded in the micropores. The feed and stripping solutions were then fed counter-currently into the tube and the shell sides, respectively. The operating time was 50 min. The outlets of the feed and stripping solutions were sampled and analyzed by high-performance liquid chromatography (HPLC).

Table 1
Properties of the hollow fiber module

Properties	Description
Materials	Polypropylene
Dimension of module (diameter × length)	6.3 × 20.3
Inside diameter of a hollow fiber	240 μm
Outside diameter of a hollow fiber	300 μm
Number of hollow fiber	35,000
Size of pore	0.05 μm
Effective surface area	1.39 m^2
Porosity	30%
Area per unit volume	29.3 cm^2/cm^3

The chromatographic procedure was carried out using an Ultron ES-OVM, ovomucoid chiral column (5 μm, 4.6 x 150 mm) (Agilent 1). The chromatographic system consisted of an Agilent1 1100 Compact LC series (Agilent Technologies, Palo Alto CA, USA), equipped with a built-in solvent degasser, quaternary pump, column compartment, photodiode array detector with variable wavelength, and auto sampler. Data analysis was carried out using ChemStation1 version B.04.01 software (Agilent). The analysis was performed following U.S. Patent No 6646131 B2 [20].

Extraction and stripping percentages were calculated from Eqs. (3) and (4)

$$\%\ \text{extraction} = \frac{C_{f,in} - C_{f,out}}{C_{f,in}} \times 100 \quad (3)$$

$$\%\ \text{stripping} = \frac{C_{s,out}}{C_{f,in}} \times 100 \quad (4)$$

where $C_{f,in}$ and $C_{f,out}$ are the inlet and outlet feed concentration of (*S*)-amlodipine (mmol/L), respectively, and $C_{s,out}$ is the outlet stripping concentration of (*S*)-amlodipine (mmol/L).

3.4. Central composite design

Four factors with five levels of central composite design (CCD) for each factor [21] was used in this study to investigate and optimize the effect of enantioseparation process variables as the pH effects of feed solution (3–7, X_1), the concentration of (+)-DBTA (1–5 mmol/L, X_2), temperature (20–60ºC), and the flow rates of feed and stripping solution (50–250 mL/min, X_4) on the maximum extraction and stripping of (*S*)-amlodipine. The process variables and their ranges were chosen from preliminary experimental results.

The process factors were each varied in five levels as shown in Table 2 with +α, -α (axial points), +1, -1 (factorial points), and 0 (central point). The α-values were 2.00. The required number of experiments for the estimation of four process parameters was 31 with 16 experiments (factorial points), 8 experiments (axial points), and 7 experiments (central point). The factor level values are shown in Table 3.

The regression equation of the second order polynomial model is presented in Eq. (5)

$$Y = \beta_0 + \sum_{j=1}^{k} \beta_j X_j + \sum_{j=1}^{k} \beta_{jj} X_j^2 + \sum_{j=1}^{k} \beta_j X_j + \sum_{i=1}^{k} \sum_{j=i+1}^{k} \beta_{ij} X_i X_j \quad (5)$$

where *Y* is the response, X_i and X_j are variables (*i* and *j* from 1 to *k*), β_j, β_{jj}, and β_{ij} are the coefficients of linear, quadratic and the second order terms, respectively, and *k* is the number of independent variables (*k* = 4 in this study).

Minitab V.17.0 program was used to calculate these coefficients. The significant factors and their interactions were determined by analysis of variance (ANOVA) (Table 3). Optimization was performed by the response surface and regression equation which correlated with the significant factors.

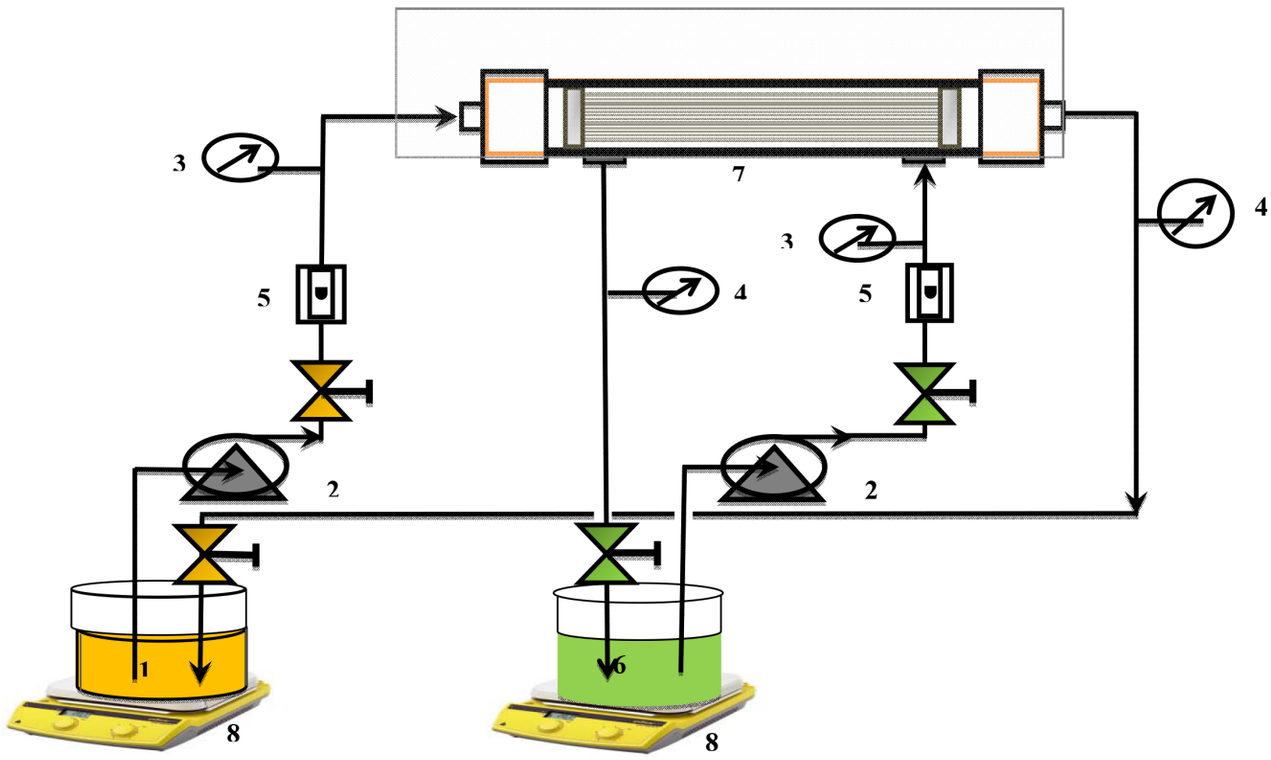

Fig. 3. Schematic counter-current flow diagram for circulated mode operation of a hollow fiber supported liquid membrane system. 1. Feed solution tank 2. Gear pump 3. Inlet pressure gauges 4. Outlet pressure gauges 5. Flow meters 6. Stripping solution tank 7. Hollow fiber module 8. heater.

4. Results and discussion

4.1. Effect of individual factors

The results of the four individual effects on extraction and stripping are shown in Figs. 4a and 5a, respectively. At pH below 5.5, the percentages of extraction and stripping were higher as pH (X_1) was increased because when pH was increased, it would increase the ionized forms of amlodipine. The enantiomers of amlodipine are expected to be ionized at pH 5.0 because the pKa of amlodipine is 8.6 [7,22]. However, at pH above 5.5 as pH increased, it would decrease of extractability and also the percentage of stripping for (*S*)-amlodipine because (*R*)-amlodipine could compete and bind to the extractant. According to the effect of (+)-DBTA concentration (X_2), the initial increase in the extraction occurred with the rise in (+)-DBTA concentration. This led to a forward shift of the extraction reaction, resulting in the formation of extracted complexes and increasing the concentration gradient along the membrane thickness. However, when (+)-DBTA concentration exceeding 1.5 mmol/L ($X_2 = -1.5$), the extractability decreased because the viscosity of the membrane phase became significant. This resulted in the increase of the liquid membrane resistance toward the diffusion of the complex species [23]. The latter was due to the diffusion coefficient of the complex across the membrane, which was inversely proportional to the viscosity, according to Wilke-Chang correlation in Eq. (6) [24].

Table 2
Variable and their level for central composite design

Factor	Factor level					Unit
	–2	–1	0	1	2	
pH of feed solution (X_1)	3.0	4.0	5.0	6.0	7.0	–
Conc. of (+) –DBTA (X_2)	1.0	2.0	3.0	4.0	5.0	mmol/L
Temperature (X_3)	20.0	30.0	40.0	50.0	60.0	°C
Flow rates of feed and srtipping solutions (X_4)	50.0	100.0	150.0	200.0	250.0	mL/min

$X_1 = (x_1 - 5)/1$; $X_2 = (x_2 - 3)/1$; $X_3 = (x_3 - 40)/10$; $X_4 = (x_4 - 150)/50$ x_i means actual value and X_i means code value.

$$D = \frac{7.4 \times 10^{-8} (\Phi_B M_B)^{0.5} T}{\mu_B V_A^{0.6}} \quad (6)$$

where D_{AB} is the diffusivity of solute A in solvent B (cm²/s), T is the temperature (K), M_B is the molecular weight of the solvent μ_B is the solvent viscosity (cP), Φ_B is the association factor for the solvent, which is 1.0 for unassociated solvents

Table 3
Central composite design factors and the responses

STD No.	X_1	X_2	X_3	X_4	% extraction	% stripping
1	–1	–1	–1	–1	81.2	75.1
2	1	–1	–1	–1	80.3	74.1
3	–1	1	–1	–1	65.1	58.8
4	1	1	–1	–1	80.9	74.6
5	–1	–1	1	–1	85.5	79.5
6	1	–1	1	–1	81.3	75.0
7	–1	1	1	–1	70.6	64.0
8	1	1	1	–1	82.3	76.5
9	–1	–1	–1	1	78.9	72.2
10	1	–1	–1	1	77.9	71.5
11	–1	1	–1	1	66.0	59.9
12	1	1	–1	1	84.7	78.9
13	–1	–1	1	1	84.0	78.0
14	1	–1	1	1	76.0	69.8
15	–1	1	1	1	71.8	65.8
16	1	1	1	1	79.9	73.8
17	–2	0	0	0	71.6	65.4
18	2	0	0	0	72.3	66.2
19	0	–2	0	0	80.0	73.6
20	0	2	0	0	76.0	74.2
21	0	0	–2	0	80.0	73.8
22	0	0	2	0	84.0	78.1
23	0	0	0	–2	76.6	70.1
24	0	0	0	2	72.0	66.1
25	0	0	0	0	82.5	76.4
26	0	0	0	0	81.9	75.8
27	0	0	0	0	82.4	76.2
28	0	0	0	0	82.4	76.2
29	0	0	0	0	82.9	76.9
30	0	0	0	0	82.5	76.4
31	0	0	0	0	82.1	76.1

such as hydrocarbons, and V_A is the molar volume of the solute *A* at its boiling temperature (mL/mol).

Increase in temperature (X_3) accelerated the rate of extraction and stripping reactions. Lastly, the increase of flow rates of feed and stripping solutions (X_4) resulted in lower contact time of the relevant molecules in the reaction in the hollow fiber module. Therefore, the extraction and stripping decreased [25].

4.2. Effect of interaction between the factors

The interactions between each of the factors on the extraction and stripping are shown in Figs. 4b and 5b, respectively. Almost every factor, X_1, X_2, X_3, and X_4, had no interaction between each factor because the curves were almost parallel. There was an interaction between the pH of feed solution (X_1) and (+)-DBTA concentration (X_2). When the concentration

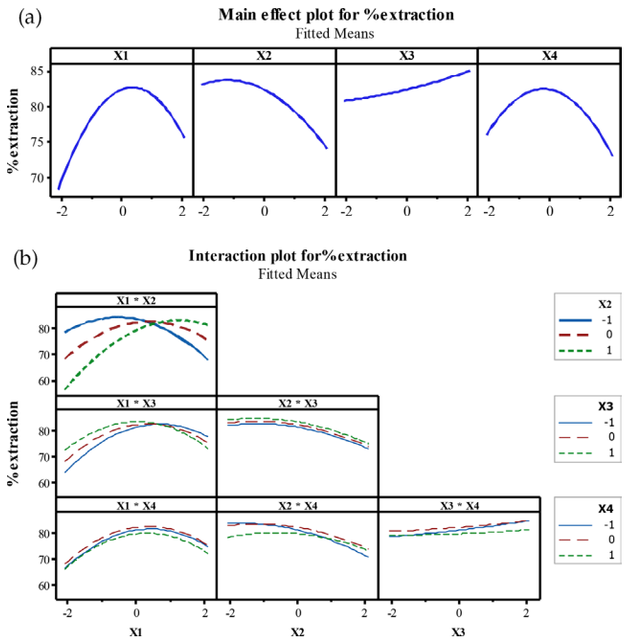

Fig. 4. Plot of the effect of pH effects of feed solution (X_1), (+)–DBTA (X_2) concentration, Temperature (X_3), and flow rates of feed and stripping solutions (X_4) on the extraction of (*S*)-amlodipine. (4a) the main effect plots and (4b) the interaction plots.

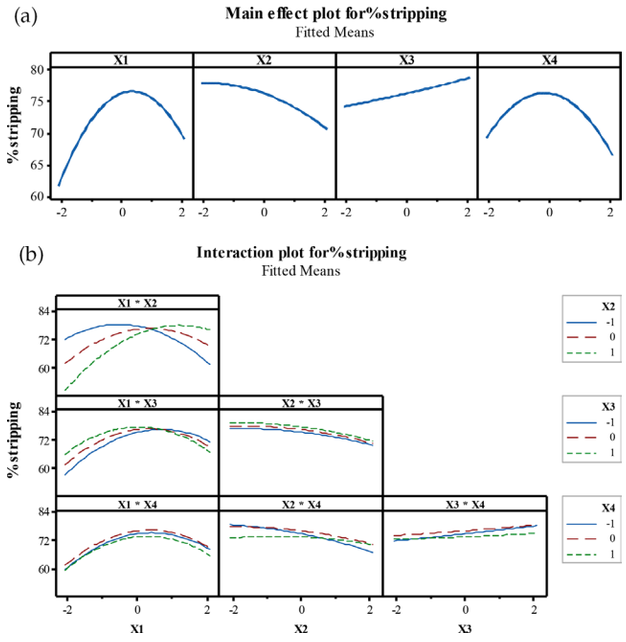

Fig.5. Plot of the effect pH effects of feed solution (X_1), (+)–DBTA (X_2) concentration, Temperature (X_3), and flow rates of feed and stripping solutions (X_4) on stripping of (S)-amlodipine. (5a) the main effect plots and (5b) the interaction plots.

of (+)-DBTA (X_2) was low (code = –1), an increase of pH (X_1) resulted in a slight increase of extraction because of insufficient (+)-DBTA available to react with high protonated amlodipine [7]. Conversely, when the concentration of (+)-DBTA was high (code:1) the extraction abruptly increased with increasing pH (X_1) because the high concentration of protonated amlodipine reacted with high concentration of (+)-DBTA. The extraction reaction shifted to the right side of Eq. (1).

4.3. Significant factors and statistical analysis

A second-order polynomial regression equation was fitted to the experimental results to develop a mathematical model to assist in predicting the percentages of extraction (Y_1) and stripping (Y_2). The developed regression model obtained in terms of coded factors is given in Eqs. (7) and (8). High R^2 of 0.924 and 0.900, respectively, clearly demonstrated model precision in exhibiting the relationship between the response and independent variables [26].

$$\begin{aligned} Y_1 = {} & 82.386 + 1.733X_1 - 2.158X_2 + 1.017X_3 - 0.717X_4 \\ & - 2.386X_1^2 - 0.874X_2^2 + 0.126X_3^2 - 1.799X_4^2 \\ & + 4.275X_1X_2 - 1.562X_1X_3 - 0.288X_1X_4 \\ & - 0.037X_2X_3 + 0.938X_2X_4 - 0.500X_3X_4 \end{aligned} \tag{7}$$

$$\begin{aligned} Y_2 = {} & 76.286 + 1.771X_1 - 1.737X_2 + 1.079X_3 - 0.654X_4 \\ & - 2.491X_1^2 - 0.466X_2^2 + 0.046X_3^2 - 1.916X_4^2 \\ & + 4.356X_1X_2 - 1.581X_1X_3 - 0.294X_1X_4 \\ & - 0.094X_2X_3 + 1.044X_2X_4 - 0.469X_3X_4 \end{aligned} \tag{8}$$

where Y_1 and Y_2 are the responses for percentages of extraction and stripping, respectively. Analysis of variance (ANOVA) was used to analyze the experimental data and results are listed in Table 4. The p-value of X_4, X_3^2, X_1X_4, X_2X_3, X_2X_4, and X_3X_4 in Eq. (7), and the p-value of X_4, X_2^2, X_3^2, X_1X_4, X_2X_3, X_2X_4, and X_3X_4 in Eq. (8) were higher than 0.05. Thus, these effects were not significant with 95% confidence [21]. Therefore, these terms were removed from the regression equations which were rewritten as Eqs. (9) and (10).

$$\begin{aligned} Y_1 = {} & 82.386 + 1.733X_1 - 2.158X_2 + 1.017X_3 - 2.386X_1^2 \\ & - 0.874X_2^2 - 1.799X_4^2 + 4.275X_1X_2 - 1.562X_1X_3 \end{aligned} \tag{9}$$

$$\begin{aligned} Y_2 = {} & 76.286 + 1.771X_1 - 1.737X_2 + 1.079X_3 - 2.491X_1^2 \\ & - 1.916X_4^2 + 4.356X_1X_2 - 1.581X_1X_3 \end{aligned} \tag{10}$$

Table 4
Analysis of variance (ANOVA)

Source	d_f	% Extraction				Stripping			
		SS	MS	F value	P-value	SS	MS	F value	P-value
Model	14	819.775	58.555	13.90	0.000	815.023	58.216	10.38	0.000
Linear	4	221.042	55.260	13.12	0.000	185.935	46.484	8.29	0.001
X_1	1	72.107	72.107	17.12	0.001	75.260	75.260	13.42	0.002
X_2	1	111.802	111.802	26.54	0.000	72.454	72.454	12.92	0.002
X_3	1	24.807	24.807	5.89	0.027	27.950	27.950	4.98	0.040
X_4	1	12.327	12.327	2.93	0.106	10.270	10.270	1.83	0.195
Square	4	247.853	61.963	14.71	0.000	262.984	65.746	11.72	0.000
X_1^2	1	162.797	162.797	38.65	0.000	177.470	177.470	31.64	0.000
X_2^2	1	21.819	21.819	5.18	0.037	6.216	6.216	1.11	0.308
X_3^2	1	0.458	0.458	0.11	0.746	0.061	0.061	0.01	0.918
X_4^2	1	92.497	92.497	21.96	0.000	105.001	105.001	18.72	0.001
Interaction	6	350.880	58.480	13.88	0.000	366.104	61.017	10.88	0.000
X_1X_2	1	292.410	292.410	69.42	0.000	303.631	303.631	54.14	0.000
X_1X_3	1	39.062	39.062	9.27	0.008	40.006	40.006	7.13	0.017
X_1X_4	1	1.323	1.323	0.31	0.583	1.381	1.381	0.25	0.627
X_2X_3	1	0.022	0.022	0.01	0.943	0.141	0.141	0.03	0.876
X_2X_4	1	14.062	14.062	3.34	0.086	17.431	17.431	3.11	0.097
X_3X_4	1	4.000	4.000	0.95	0.344	3.516	3.516	0.63	0.440
Error	16	67.393	4.212			89.734	5.608		
Lack of fit	10	66.784	6.678	65.84	0.000	89.046	8.905	77.59	0.000
Pure error	6	0.609	0.101			0.689	0.115		
Total	30	887.168		$R^2 = 0.924$		904.757		$R^2 = 0.900$	

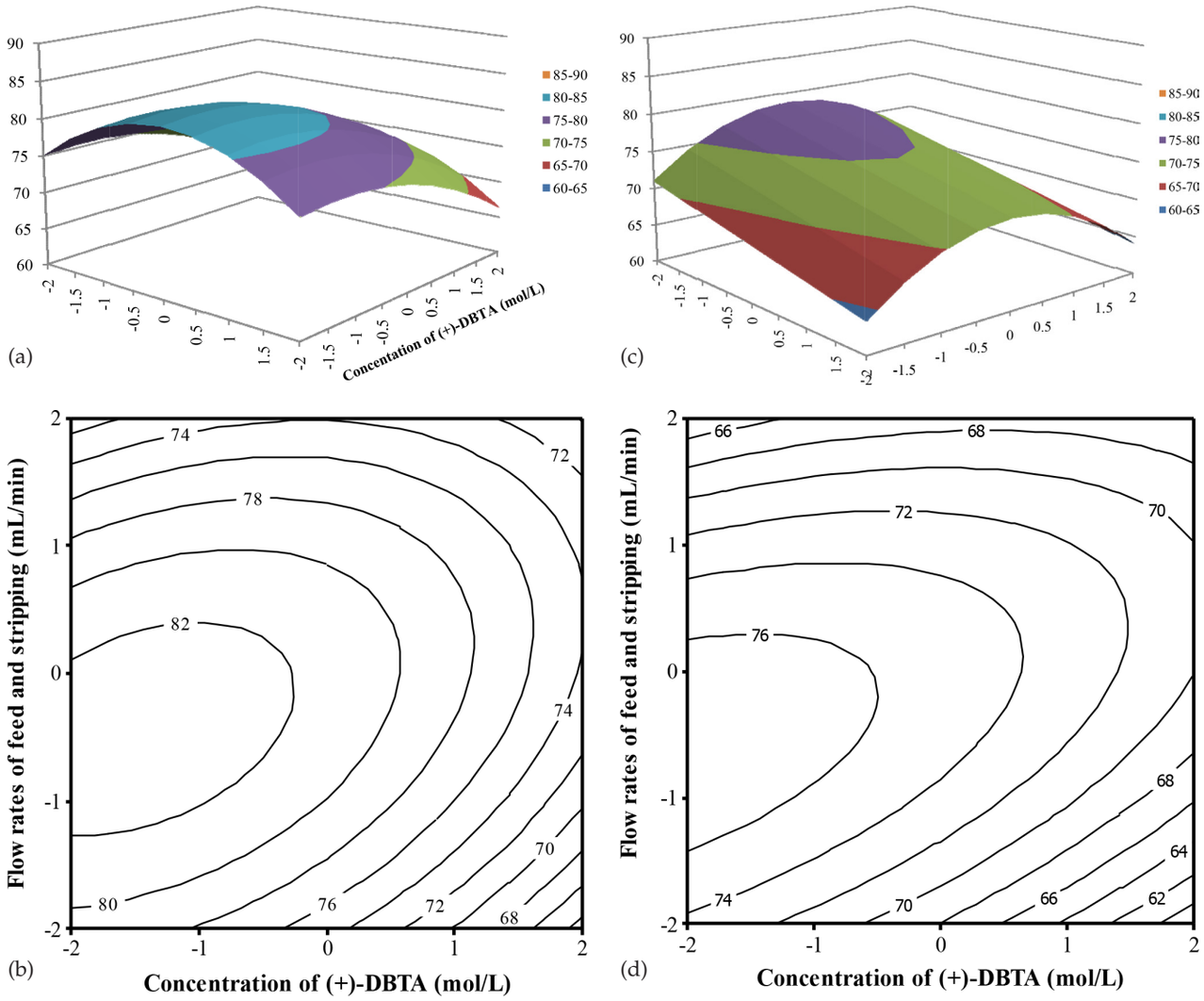

Fig. 6. Contour plots showing the effect of concentration of (+)–DBTA (X_2) and flow rates of feed and stripping solutions (X_4) and stripping (6b) of (S)-amlodipine. (6a) Response surface of extraction, (6b) Contour plot of extraction, (6c) Response surface of stripping, (6d) Contour plot of stripping.

4.4. Optimization of enantioseparation

The four operating factors of the pH of feed solution (X_1), concentration of (+)-DBTA (X_2), temperature (X_3), and flow rates of feed and stripping solution (X_4) were optimized using response surface methodology. A fitted regression equation was used to generate response surface and contour plots to visualize the relationship between response and experimental levels of process variables and deduce the optimal condition. Fig. 6a, 6b, and 6c, 6d show the response surface and contour plots for the extraction and stripping of (s)-amlodipine generated from Eqs. (9) and (10), respectively. The pH of the feed solution (X_1) was fixed at 5.0 (code: 0), and the temperature (X_3) was fixed at 30.0°C (code: –1) for convenient operation. The contour plots of extraction and stripping in Fig. 6b and 6d were superimposed. From observation, point A in the overlapping regions was selected as the optimum conditions for the extraction of ≥82.0% and stripping ≥76.0% as shown in Fig. 7. Therefore, the concentration of (+)-DBTA at 1.5 mmol/L, (X_2 = –1.5) and flow rates of feed and stripping solution of 125 mL/min (X_4 = –0.5) were selected as the optimum condition.

4.5. Validation of the optimized condition

The optimized condition (X_2 = –1.5, X_4 = –0.5) process predicted from section 4.4 was validated, and the percentages of extraction and stripping at different flow rates of feed and stripping solution are shown in Fig. 8. The results indicated that when the flow rates of feed and stripping solution increased from 100 to 300 mL/min, the percentages of extraction and stripping were around

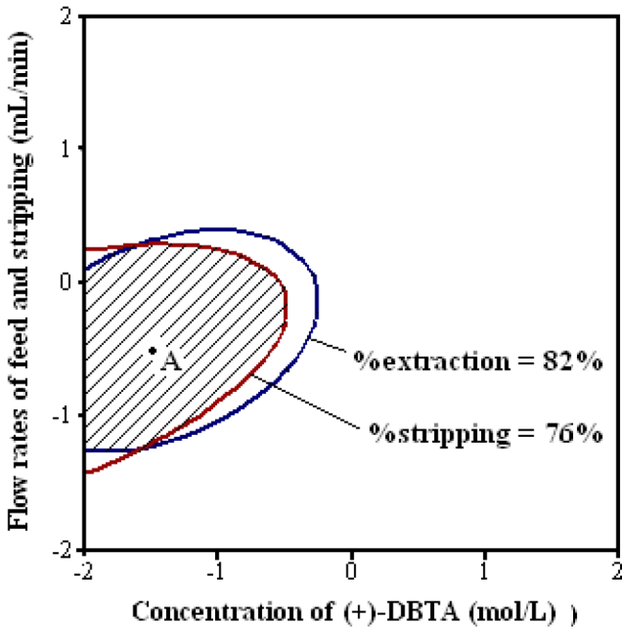

Fig. 7. Superimposed contour plots showing the shaded overlapping area for which %extraction ≥ 82% and %stripping ≥ 76%.

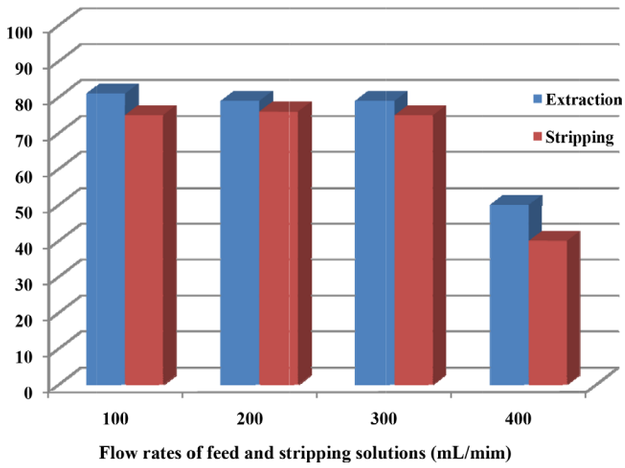

Fig. 8. The relation between flow rates and percentages of extraction and stripping.

80 and 75, respectively. The experimental values were, therefore, in agreement with the predicted values in Eqs. (9) and (10), and the optimized condition predicted by CCD and response surface was satisfactory. However, when the flow rate was 400 mL/min, both extraction and stripping percentages suddenly decreased because the flow rate was too high and the capillary force which immobilized the liquid membrane at the pore-mouth was destroyed. In this case, the extraction percentages of 50 and stripping percentages of 40 were meaningless. Therefore, according to this study, a flow rate between 100 and 300 mL/min was recommended for the separation of (*S*)-amlodipine by hollow fiber supported liquid membrane.

5. Conclusions

(*S*)-amlodipine can be selectively extracted from racemic amlodipine in pharmaceutical wastewater. Flow rates and some interaction terms were insignificant factors. A concentration of (+)-DBTA of 3.5 mmol/L and flow rates of feed and stripping solution of 175 mL/min were determined as the optimum condition, while the pH of the feed solution and temperature were fixed at 5.0 and 30°C, respectively.

Acknowledgments

This research is supported by Rachadapisek Sompote Fund for Postdoctoral Fellowship, Chulalongkorn University. The authors deeply appreciate the support under The Institutional Research Grant (The Thailand Research Fund), IRG 5780014, and Chulalongkorn University, Contract No. RES_57_411_21_076 as well. The authors are sincerely grateful to the Department of Chemical Engineering, Faculty of Engineering and Industrial Technology, Silpakorn University. Thanks are also given to the Separation Laboratory, Department of Chemical Engineering, Faculty of Engineering, Chulalongkorn University, Bangkok, Thailand, for chemical and apparatus support, and to the Government Pharmaceutical Organization (GPO), Thailand, for kindly supplying active pharmaceutical ingredients and all instruments for analysis and measurement.

References

[1] N. Turgan, S.Habif, C.G. Kabaroğlu, I. Mutaf, D. Özmen, O. Bayindir, A. Uysal, Effects of the calcium channel blocker amlodipine on serum and aortic cholesterol, lipid peroxidation, antioxidant status and aortic histology in cholesterol-fed rabbits, J. Biomed. Sci., 10 (2003) 65–72.

[2] H.W. Lee, S.J. Shin, H. Yu, S.K. Kang, C.L. Yoo, A novel chiral resolving reagent, bis ((S)-mandelic acid)-3-nitrophthalate, for amlodipine racemate resolution: Scalable synthesis and resolution process Org. Process Res. Dev., 13 (2009)1382–1386.

[3] Y.H. Sun, L. Fang, M. Zhu, W. Li, P. Meng, L. Li, Z.G. He, A drug-in-adhesive transdermal patch for S-amlodipine free base: in vitro and in vivo characterization. Int. J. Pharm., 382 (2009) 165–171.

[4] D.M. Gotrane, R.D. Deshmukh, P.V. Ranade, S.P. Sonawane, B.M. Bhawal, M.M. Gharpure, M.K. Gurjar, A novel method for resolution of amlodipine, Org. Process Res. Dev., 14 (2010) 640–643.

[5] B. Streel, C. Laine, C. Zimmer, R. Sibenaler, A. Ceccato, Enantiomeric determination of amlodipine in human plasma by liquid chromatography coupled to tandem mass spectrometry, J. Biochem. Biophys. Methods.,54 (2002) 357–368.

[6] J. Luksa, D.J.B. Podobnik, B. Furlan, M. Kremser, Semi-preparative chromatographic purification of the enantiomers S-(–)-amlodipine and R-(+)-amlodipine, J.B. Chromatogr., 693 (1997) 367–375.

[7] M. Zandkarimi, A. Shafaati, S.M. Foroutan, C.A. Lucy, Rapid enantioseparation of amlodipine by highly sulfated cyclodextrins using short-end injection capillary electrophoresis, DARU, 17 (2009) 269–276.

[8] V. Kislik, Principles and Applications in Chemical Separations and Wastewater Treatment, Elsevier Science, 2009.

[9] B.L. Avinash, S.K. Prashant, Selective recovery of tungsten from printed circuit board recycling unit wastewater by using emulsion liquid membrane process, J. Water Process Eng., 8 (2015) 75–81.

[10] A. Uheida, Y. Zhang, M. Muhammed. (2004). Transport of palladium(II) through hollow fiber supported liquid membrane facilitated by nonylthiourea J. Membr. Sci., 241 (2004) 289–295.
[11] D. Huang, K. Huang, S., Chen, S. Liu, J. Yu, Rapid reaction-diffusion model for the enantioseparation of phenylalanine across hollow fiber supported liquid membrane. Sep. Sci. Technol., 43 (2008) 259–272.
[12] Z. Weidong, C. Chunhua, H. Zisu, Transport study of Cu(II) through hollow fiber supported liquid membrane. Chin. J. Chem. Eng., 18(1) (2010) 48–54.
[13] N. Leepipatpiboon, U. Pancharoen, P. Ramakul, Separation of Co(II) and Ni(II) from thiocyanate media by hollow fiber supported liquid membrane containing Alamine300 as carrier — investigation on polarity of diluent and membrane stability, Korean J. Chem. Eng., 30 (2013) 194–200.
[14] A.W. Lothongkum, Y. Khemglad, N. Usomboon, U. Pancharoen,. Selective recovery of nickel ions from wastewater of stainless steel industry via HFSLM, J. Alloys. Compd., 476 (2009) 940–949.
[15] P. Ramakul, T. Supajaroon, T. Prapasawat, U. Pancharoen, A.W. Lothongkum, Synergistic separation of yttrium ions in lanthanide series from rare earths mixture via hollow fiber supported liquid membrane., J. Ind. Eng. Chem., 15 (2009) 224–228.
[16] M.S. Manna, P. Saha, A.K. Ghoshal, Separation of medicinal catechins from tea leaves (Camellia sinensis) extract using hollow fiber supported liquid membrane (HF- SLM) module, J. Membr. Sci., 471 (2014) 219–226.
[17] N. Sunsandee, N. Leepipatpiboon, P. Ramakul, T. Wongsawa,U. Pancharoen, Selective enantioseparation of racemic amlodipine by biphasic recognition chiral separation system, Sep. Purif. Technol., 102 (2013) 50–61.
[18] N. Sunsandee, N. Leepipatpiboon, P. Ramakul, U. Pancharoen, The selective separation of (*S*)-amlodipine via a hollow fiber supported liquid membrane: Modeling and experimental verification Chem. Eng. J., 180 (2012) 299–308.
[19] A. Mohammadi, N. Rezanour, M.A. Dogaheh, F.G. Bidkorbeh, M. Hashem, R.B.A. Walker, A stability-indicating high performance liquid chromatographic (HPLC) assay for the simultaneous determination of atorvastatin and amlodipine in commercial tablets, J. Chromatogr. B. Analyt. Technol. Biomed. Life. Sci., 846 (2007) 215–221.
[20] Y.S. Chung, M.C. Ha, (2003) Resolution of the enantiomers of amlodipine. US Patent Application 2003=6646131 B2, 11 November.
[21] D.C. Montgomery, Design and Analysis of Experiments, John Wiley and Sons Inc. 2013.
[22] N. Sunsandee, N. Leepipatpiboon, P. Ramakul, Selective enantioseparation of levocetirizine via a hollow fiber supported liquid membrane and mass transfer prediction Korean J. Chem. Eng., 30 (2013) 1312–1320.
[23] R. Ruhela, S. Panja, J.N. Sharma, B.S. Tomar, S.C. Tripathi, R.C. Hubli, A.K. Suri, Facilitated transport of Pd (II) through a supported liquid membrane (SLM) containing N,N,N′,N′-tetra-(2-ethylhexyl) thiodiglycolamideT (2EH) TDGA: A novel carrier. J. Hazard. Mater., 229 (2012) 66–71.
[24] C.R. Wilke, P. Chang, Correlation of diffusion coefficients in dilute solutions. AIChE., 1 (1955) 264–270.
[25] P. Ramakul, W. Pattaweekongka, U. Pancharoen, Selective separation of trivalent and tetravalent lanthanide from mixture by hollow fiber supported liquid membrane. J. Chin. Inst. Chem. Engrs., 36 (2005) 1–7.
[26] M.J. Prakash, S. Manikandan, N.C. Vigna, R. Dinesh. Ultrasound assisted extraction of bioactive compounds from *Nephelium lappaceum* L. fruit peel using central composite face centered response surface design, Arabian. J. Chem., (2013).